Desalination and Water Treatment
www.deswater.com
doi: 10.5004/dwt.2020.26343

205 (2020) 53–62
November

Application of high performance FO nanofibers based membrane for model and real seawater desalination

Raed M. El Khaldi[a,b], Mehmet E. Pasaoglu[a,c], Yusuf Z. Menceloglu[d], Reyhan Ozdogan[e], Mithat Celebi[e], Mehmet A. Kaya[e], Ismail Koyuncu[a,c,*]

[a]*Civil Engineering Faculty, Environmental Engineering Department, Istanbul Technical University, 34469 Maslak, Istanbul, Turkey, Tel. +90 285 3417/+90 285 3473; email: koyuncu@itu.edu.tr (I. Koyuncu), Tel. +970 8 2860700; emails: raedmkhaldi@iugaza.edu.ps (R.M. El Khaldi), mpasaoglu@itu.edu.tr (M.E. Pasaoglu)*
[b]*Islamic University of Gaza, Environmental and Earth Sciences Department, 108 Gaza Strip, Palestinian Authority*
[c]*National Research Center on Membrane Technologies (MEM-TEK), Advanced Technology Center, 34469 Maslak, Istanbul, Turkey*
[d]*Faculty of Engineering and National Sciences, Sabancı University, 34956 Tuzla, İstanbul, Turkey, Tel. +90 483 9000; email: yusufm@sabanciuniv.edu (Y.Z. Menceloglu)*
[e]*Engineering Faculty, Polymer Engineering Department, Yalova University, 77200 Yalova, Turkey, Tel. +90 226 8155400; emails: reyhan.ozdogan@yalova.edu.tr (R. Ozdogan), mithat.celebi@yalova.edu.tr (M. Celebi), marifkaya@yalova.edu.tr (M.A. Kaya)*

Received 24 December 2019; Accepted 10 July 2020

ABSTRACT

The performance evaluation of forward osmosis (FO) nanofibers based membranes against model solutions and real seawater were investigated. The desalination of seawater performed using 2 M NaCl as a draw solution. Performance data showed that when real seawater used as a feed solution, the newly fabricated FO membrane has a water flux of 15.1 and 49.4 LMH in both co-current FO and co-current pressure retard mode (PRO) respectively. Two different model solutions (NaCl and $MgSO_4$), have a salt concentration equal to that of the real seawater sample, were prepared to characterize the performance of the fabricated membrane against them under the same operating conditions. The flux obtained in 1.1% model NaCl in FO mode was 8 LMH, whereas in PRO mode was 54 LMH and 10.3 LMH in FO mode, whereas 45.6 LMH in PRO mode for model 1.1% $MgSO_4$ solution using 2 M NaCl solution as a draw solution. The structural parameter (*S*-value) of the sulfonated polysulfone (sPSf) thin-film-composite membrane is estimated to be 125 μm, which is considered one of the smallest values ever reported in the literature. In this manuscript, the performance study of thin-film composite (TFC-FO) nanofiber flat-sheet membrane on sPSf substrate is proven that fabricated membranes are perfectly meet the high rejection ratios whether strong enough to sustain high flux and durability through the operation.

Keywords: Forward osmosis; Desalination; Thin-film-composite membrane; Sulfonated polysulfone; Electrospining

1. Introduction

Reliance on water desalination as an efficient innovative technology getting more popular day by day to face freshwater scarcity, particularly in arid and semi-arid areas, where climatological factors assisted by the increase of population growth, urbanization, and water contamination [1]. Nowadays, membrane separation is the most widely recognized technology in the field of desalination. Reverse osmosis (RO) is the first membrane separation process introduced on the industrial scale for seawater desalination.

* Corresponding author.

Most commercial RO membranes are polymeric based thin film composite (TFC) membranes, configured in spiral-wound, hollow fiber, and tubular modules, composting of an ultra-thin separating film (normally polyamide) on the top of the porous support layer (polysulfone) which cast upon a non-woven polyester material. Normally, the synthesis of an ultra-thin separating layer can be obtained by interfacial polycondensation between poly/monomeric amines and poly/monomeric functional acid halide [2]. Even though the main task of the substrate is providing mechanical support strength for the separation layer against applying hydraulic pressure, proper fabrication techniques and material selection are a condition to form a substrate with a smooth surface, suitable for separation layer formation [3,4]. The conventional TFC membrane has a hydrophobic sponge-like polysulfone substrate [5].

Recently, forward osmosis (FO) technology gained popularity as a low energy alternative in the application of desalination [6], concentration [7], dewatering [8], power production [9] and many other fields. The best performance commercially available FO membrane is also an asymmetric TFC-FO membrane. Fundamentally, the FO process [10] uses the advantages of induced water diffusion across a semi-permeable membrane (Fig. 1). Water diffusion takes place spontaneously from a low concentration to a high concentration solution. The semi-permeable membrane performs as a barrier that allows water to pass on the other hand rejects salts and other elements.

One may be wondering, why we cannot vitally use RO membranes in the FO systems? While in the RO process, water flux is driven by applying hydraulic pressure against the osmotic pressure gradient, in the forward osmosis, water movement can occur from low concentration (the feed side) to high concentration (the draw side) in the virtue of the osmotic pressure gradient. Accordingly, unlike the RO membrane structure that needs to be thick enough to deal with prolonged exposure to applied pressure, the FO membrane should be as thin as possible to facilitate diffusion [11]. Bearing in mind that the circulation of two solutions on both sides of the FO membrane could create high salt polarization, the design of the FO membrane substrate could differ from that of RO membranes. A thinner and higher hydrophilic support layer is desirable in FO processes to enhance water flux, limit the internal concentration polarization effect and control propensity to fouling [11].

Where there is no big difference in the separation layer properties in both the RO and FO asymmetric composite membranes which would be characterized by high pure water permeability coefficient (A value) and low salt permeability coefficient (B value), the membrane structural parameter (denoted as S), which consider supporting layer property, should be as small as in the FO membranes to overcome the effect of internal concentration polarization that responsible for the sound decline of water flux in the osmotically driven membranes.

Park et al. [12] conducted a sensitivity analysis using the LH-OAT method to determine the effects of operational and membrane parameters on the performance of the FO process. Among the selected model parameters (which compromise A, B, diffusion coefficient D, S, average inlet velocity of the feed solution channel, and average inlet velocity of the draw solution channel), S and A values of the membrane are noticed to have the most influential parameters. FO process performance can be enhanced by an increase of A-value and a

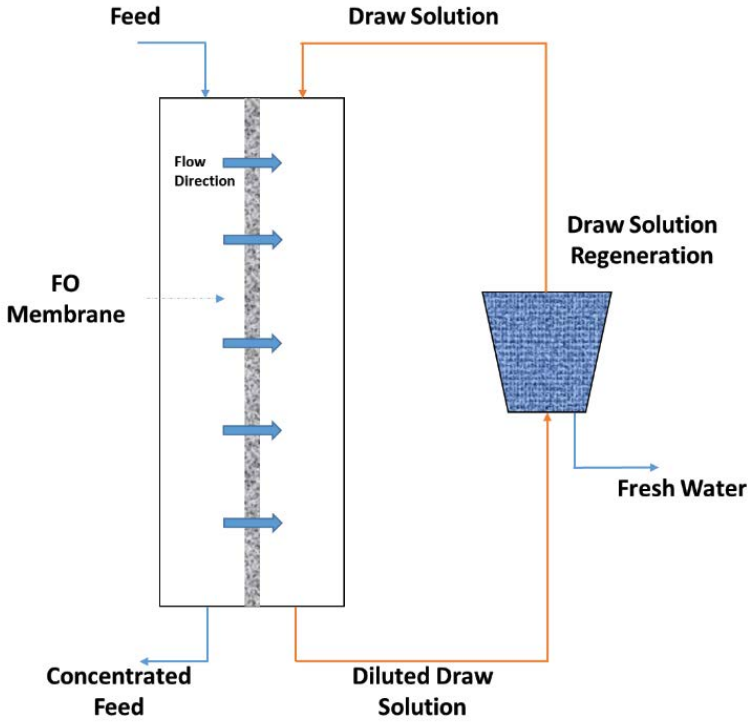

Fig. 1. Schematic diagram of a typical forward osmosis process, modified from [10].

decrease of *S*-value. These results imply that the modification of intrinsic membrane parameters (*A* and *S*) plays a more decisive role than the optimization of operating conditions.

McCutcheon and Elimelech [13] assumed that the hydrophobicity of the membrane support layer significantly limits water flux due to insufficient wetting that aggravates internal concentration polarization and obstructs water continuity. They suggested that besides the structural redesign of the FO membrane support layer, increasing its hydrophilicity would improve the performance through elevating mass transfer within the membrane. On the other hand, Widjojo et al. [14] found that the structural parameter (*S*) decreases with an increase in the sulfonated polymer ratio in membrane substrates. It is inferred that a lower internal concentration polarization (ICP) effect can be obtained when the TFC-FO membrane substrates enjoy higher hydrophilicity or porous nature for FO applications.

Recently, a new design concept was introduced to FO-TFC membranes that utilized electrospun nanofiber mate as a substrate for the ultrathin separation layer. This substrate with scaffold structure has a high porosity, interconnected pore structure, and low structural parameter.

TFC membranes supported by an electrospun nanofiber substrate have been employed in the forward osmosis process. Electrospun nanofiber fabricated originally from hydrophilic polymer shown a high swelling degree that negatively affected fiber strength and membrane integrity. To avoid this problem, non-swelling hydrophobic polymers such as polysulfone (PSf) and polyvinylidene fluoride (PVDF) were modified to be surfacially hydrophilic and fully wettable [15]. In this study, PSf was chemically modified via sulfonation to gain better hydrophilicity. The PSf selected due to its ease of availability, low cost, thermal, mechanical and chemical stability.

Commonly, in many studies, assessment of the potential use of certain FO membranes for seawater desalination carried out using distilled water as a feed solution to determine pure water permeability and the other intrinsic properties. But, the application against real seawater or more concentrated solution the membrane reveals severe underperformance. Wang et al. [16] proven that the water flux decreases when deionized water (DIO) water in the feed side is replaced by concentrated solutions and referred that to the reduction of the osmotic pressure gradient. Rather, a reduction in the overall osmotic pressure difference can be increased as the concentration in the feed and draw solutions on both membrane sides increased. This reduction can be experienced in both FO and pressure retard mode (PRO) modes, but could be more pronounced in the FO mode, because, in the FO configuration, the water permeating through the porous support layer dilutes the draw solution (DS) inside the support (named dilutive ICP/dilutive internal concentration polarization) and concentrate the feed on the dense rejection layer). Conversely, in the case of PRO mode, the solutes inside the support are concentrated (named concentrative ICP/concentrative internal concentration polarization) and that on the dense rejection are diluted [named dilutive external concentration polarization (ECP)/dilutive external concentration polarization] as the water permeates through the membrane in the PRO configuration (Fig. 2) [11,17].

It is found that, with an increase in feed concentration, the water flux difference between PRO and FO modes becomes less gradually, mainly because of the ICP that struggle water transport within the porous substrate layer [16,19].

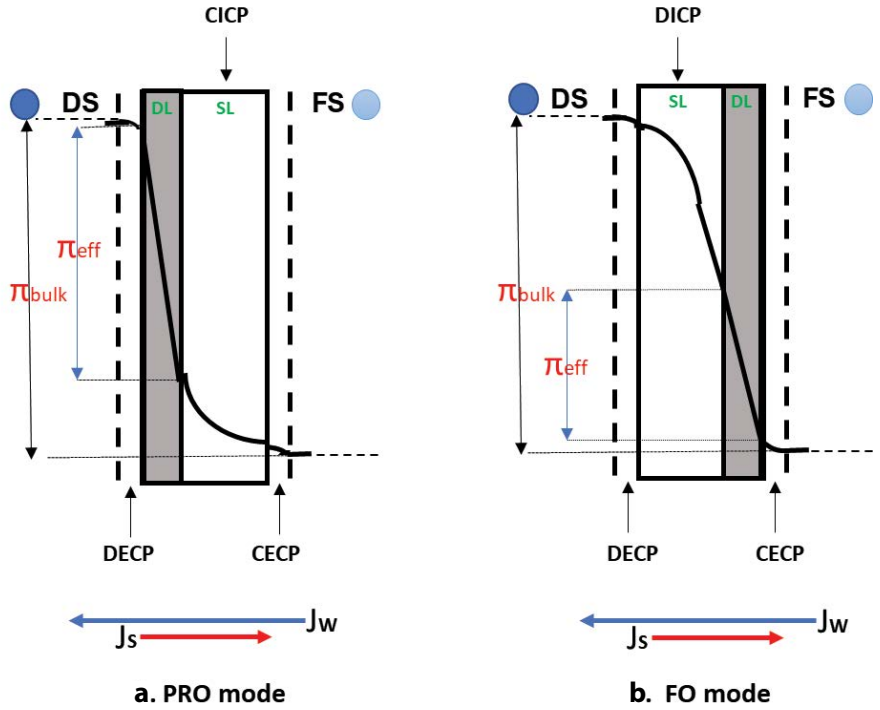

Fig. 2. Schematic diagrams of external and internal concentration polarization developed (a) in PRO operating mode, and (b) in FO operating mode (adapted from [18]).

In this study, in addition to the real seawater sample, two different synthetic solutions (NaCl and $MgSO_4$), with a salt concentration equal to that of the real seawater one, were prepared to characterize the performance of the fabricated membrane under the same operating conditions.

2. Experimental setup

2.1. Materials and methods

The materials and methods associated with the membrane fabrication and the experiments carried out in this work are described in further detail in our previous work [20] but it will be briefly explained in Fig. 3.

The dope formulations are sulfonated polysulfone (sPSf)/dimethylacetamide with a weight ratio of 30/70. NaCl and $MgSO_4$ were utilized to prepare the model seawater. The material used for the fabrication of support and dense separation layers, in addition to its amount and the source companies are listed in Table 1.

Membrane fabrication and characterization were done following the same procedure used by the teamwork that described elsewhere [20].

2.2. Forward osmosis set up

A lab-scale closed-loop FO setup was used (Fig. 4) to evaluate the fabricated membrane performance against osmotic water flux, salt permeability, and salt rejection. The operating conditions of the FO setup in both feed solutions that is, active layer-feed solution and active layer-draw solution modes are illustrated in Table 2.

The water flux, J_W, was calculated by dividing the collected volume within a certain time period by the membrane area. Reverse salt flux, J_S, is also calculated by dividing the NaCl mass flow rate by the membrane area using Eq. (1) [19,21]:

$$C_F\left(V_{F0} - J_W A_w t\right) = J_S A_m t \tag{1}$$

where C_F is the NaCl concentration in the feed, V_{F0} is the initial volume of the feed solution, J_W is the measured water flux, A_m is the membrane area, and t is time.

Evaluation of the membrane potential for seawater desalination was accomplished using synthetic solutions and real seawater. The seawater sample (15.77 ms/cm) was taken from the Bosphorus bay in February and was used as a feed solution against the 2 M NaCl draw solution. For further characterization, two synthetic NaCl and $MgSO_4$ solutions with the same concentration of the real seawater sample (15.77 ms/cm). The FO performance tests were evaluated from data collected over a 3 h period after running the experiment for 15 min to bring water flux and circulation for a stable state.

Attenuated total reflection–Fourier-transform infrared (ATR-FTIR) spectroscopy (PerkinElmer Spectrum 100 FTIR Spectrometer, United States of America) was utilized to check the successful formation of a TFC layer onto sPSf nanofiber support.

Pure water permeance, A, was measured using standard RO test methodology at three different low-pressure points, while solute permeability coefficient, B, was calculated by utilizing the water flux and salt rejection data addressed in Eq. (2) [22]:

$$B = A\left(\Delta P - \Delta\pi\right) \times \left(\frac{1}{R} - 1\right) = J_W \times \left(\frac{1}{R} - 1\right) \tag{2}$$

where B is the solute permeability (LMH), R is the rejection, A is the water permeance of the membrane (LMH bar^{-1}), ΔP is the transmembrane hydrostatic pressure (bar), and $\Delta\pi$ is the transmembrane osmotic pressure (bar).

The salt rejection rate (R, %) was calculated from Eq. (3).

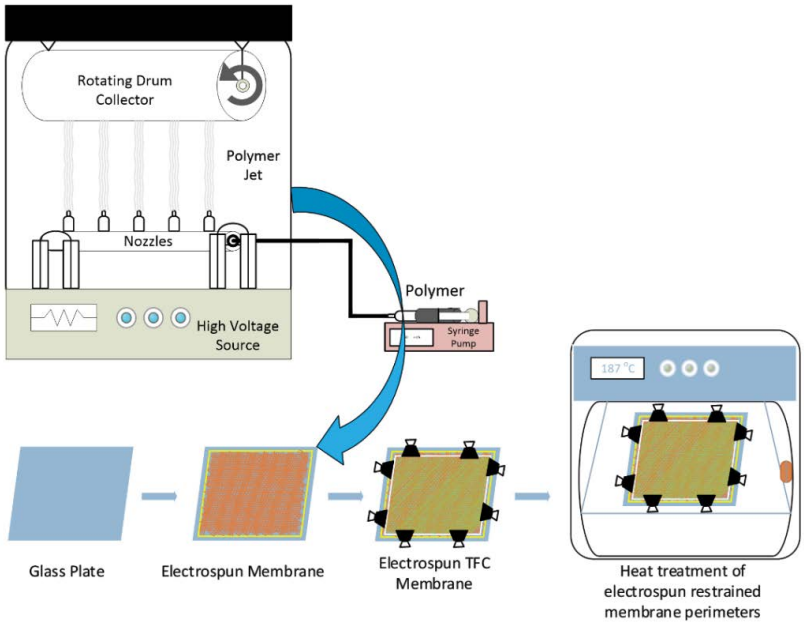

Fig. 3. Schematic diagrams membrane fabrication steps in our previous work [20].

Table 1
Chemical materials and amounts that used for the fabrication of newly developed membrane and it is source companies

Material	Symbol	Amount/100 mL	For	Source/comp.
Polysulfone	PSf	30 g	Substrate dope	Solvay, Belgium
Dimethylacetamide	DMAc	70 mL	Substrate dope	Akkim, Turkey
m-phenylene diamine	MPD	2 g	MPD solution	Merck, Germany
Triethylamine	TEA	2.75 mL	MPD solution	Merck, Germany
(+)-10-camphorsulfonic acid	CSA	2 g	MPD solution	Sigma-Aldrich, United States of America
Sodium dodecyl sulfate	SDS	0.1 g	MPD solution	Sigma-Aldrich, United States of America
1,3,5-benzenetricarbonyl trichloride	TMC	0.1 g	TMC solution	Sigma-Aldrich, United States of America
Hexane anhydrous, 95%	–	100 mL	TMC solution	Sigma-Aldrich, United States of America
Sodium chloride	NaCl	2 M	DS	Merck, Germany
		15.7 ms/cm	Synthetic seawater	
Magnesium sulfate	$MgSO_4$	15.7 ms/cm	Synthetic seawater	Merck , Germany

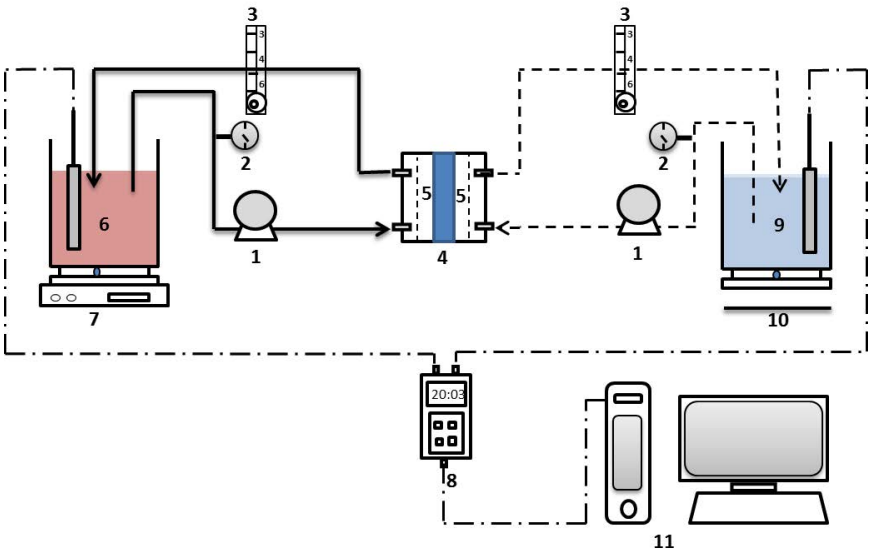

Fig. 4. Schematic diagram of the lab-scale FO setup. (1) Circulating pump; (2) flow meter; (3) flow meter; (4) FO membrane; (5) flow chamber of the FO test unit (membrane cell); (6) draw the solution reservoir; (7) magnetic stirrer; (8) electrical conductivity meter; (9) feed solution container; (10) weighing balance; (11) computer.

$$R = 1 - \left[\left(\frac{m}{L}/M\right)\right] \quad (3)$$

where m, L, and M are mole NaCl transferred to feed, water removed, and molarity of draw solution, respectively.

3. Results and discussion

3.1. Intrinsic separation properties and performance parameters (osmotic water flux, salt permeability, and salt rejection)

The performance of FO membranes is routinely quantified by three parameters which are (1) water flux, J_W (LMH), (2) reverse salt flux, J_S (gMH), and (3) salt rejection rate (%). These parameters mainly rely on the intrinsic transport properties of the membrane TFC layer (represented by the water permeability coefficient A and salt permeability coefficient B) and substrate structure (represented by structural parameter-S-value), and to a fewer extent on other factors.

Detailed information about the TFC layer intrinsic properties and performance parameters of the newly fabricated membrane are shown in Table 3. The intrinsic water permeability coefficient (A) was tested under three different hydraulic pressures ranging from 0.3–1.0 bar (4.35–14.5 psi) by a dead-end Sterlitech (United States of America) cell under constant stirring, while the salt permeability coefficient (B), salt rejection rate, pure water flux, and reverse salt flux were determined/calculated by FO setup in the FO co-current mode using 1.0 M NaCl as a DS and DIO as an feed water.

Table 2
FO setup operation conditions used to characterize the membrane in both FO and PRO modes

	Circulation rate on FS	Circulation rate on DS	Initial FS volume	Initial DS volume	Effective membrane area	Temperature
FO mode	600 rpm = 16.12 cm/s	280 rpm = 7.86 cm/s	1.5 L	0.5 L	0.0058 m^2	Room temperature
PRO mode	280 rpm = 7.86 cm/s	600 rpm = 16.12 cm/s	1 L	0.8 L	0.0058 m^2	Room temperature

Table 3
Transport properties and structure parameters of the fabricated sPSf-TFC membrane

Membrane	Water flux, J_W (FO) (LMH)	Reverse salt flux, J_S (FO) (gMH)	J_S/J_W (g/L)	J_W/J_S (L/g)	Rejection (%)	Water per*, A (LMH bar^{-1})	Salt per**, B (LMH)	(A/B) FO (bar^{-1})	Draw solution
TFC-FO flat-sheet membrane on sPSf	65.7	2.5	0.038	26.3	99.54	4.97	0.287	17.31	1.0 M NaCl

*1,000 ppm NaCl as the feed solution in the RO test;
**1.0 M NaCl as the draw solution and deionized water as feed in the FO mode.

All tests were performed three times in order to eliminate experimental errors. In this membrane, the TFC layer revealed a very high A value of 4.97 (LMH bar^{-1}) and a low B value of 0.287 (LMH) which results in a high J_W/J_S ratio of 26.3. A larger A/B ratio indicates a better filtration performance and a lesser solute loss per unit of water produced is lower.

3.2. Estimation of structural parameters

In most of the studies, membrane research groups used the S parameter to evaluate the membrane's eligibility in FO processes. The S parameter is related to the substrate's thickness (t), porosity (ε), and tortuosity (τ) ($S = \tau \times t/\varepsilon$) [13]. The smaller the S-value, the better the diffusion of the solutes inside the porous substrate, and the more limited the ICP effect on membrane performance become. To forward the performance of the FO membrane, scientists should target the TFC-FO membrane with a substrate S-value of less than 300 μm. Recently developed lab-made nanofiber-based TFC-FO membranes showed interesting low S parameter values Table 4.

In this study, ForwardOsmosisTech's S-value calculator was used to estimate the new fabricated membrane S-value (Eq. (4)) [23]. The calculator is based on the following S-value equation for the FO membrane operating in FO mode.

$$S = \left(\frac{D}{J_W}\right) \times \ln \frac{\left(B + A \times \prod_{D,B}\right)}{\left(B + J_W + A \times \prod_{F,M}\right)} \quad (4)$$

where D is the diffusion coefficient for the NaCl draw solution used for J_W determination. $\prod_{D,B}$ is the osmotic pressure of the bulk draw solution. $\prod_{F,M}$ is the osmotic pressure of the feed solution close to the membrane surface. The values of A, B, J_W, aforementioned in the table above fed to online calculators, as well as water temperature (298 K) and molarity of draw solution used during J_W determination (1 M). The newly developed membrane has S-values of 125 μm. This favorable small value reflects high solute diffusivity inside the substrate matrix and a restricted effect of ICP phenomena.

3.3. Evaluation of FO membrane performance

3.3.1. Performance of FO membrane using real seawater as a feed solution

To examine the potential use of the newly developed membrane for seawater desalination, a water sample (15.77 ms/cm) taken from the Bosphorus Bay/Istanbul was used as a feed solution against the 2 M NaCl draw solution. The seawater sample was subjected to microfiltration before use to avoid any potential effect of the suspended material on the membrane performance. Water flux was measured in co-current cross-flow for both RO and PRO mode. Flux data logged for 3 h and the average value is taken to express mean water flux. As seen in Table 5, the newly developed membrane shows a higher water flux of 15.11 and 49.44 LMH under both FO and PRO modes respectively. When seawater is used as a feed solution in place of DIO, water fluxes decrease in both PRO and FO modes due to the reduction of the overall osmotic pressure difference between the feed and the draw solution.

Even though the modeling studies assume that transport phenomena inside the porous substrates with sponge and finger-like structures have a linear relationship between the osmotic pressure and salt concentration, particularly in the dilute solutions, this relation is no longer valid in the case of concentrated solutions due to its salt gradient within the substrate matrix. Unlike previously mentioned membranes substrate structures, this membrane with scaffold substrate showed a convenient proportionality between water flux and draw solution concentration during the FO operation when both sides of the membrane have a high concentration as seen from Fig. 5.

Reduction of initial water flux (25 LMH in co-current PRO and 89 LMH in co-current PRO) related mainly to the decline of draw solution concentration. This decrease of

Table 4
Structural parameter of recently developed lab-made nanofiber-based TFC-FO membranes

Substrate	Modification route	S (μm)	Reference
PSf	Sulfonation	125	This work
PAN	Mesoporous silica nanoparticles	65	[24]
PAN	Adding NaCl in coagulation bath	84.35	[25]
PVDF	Surface modified/hydrophilization using polyvinyl alcohol	154	[26]
PAN	–	168	[27]
PVDF	Bentonite nanoclay	187.9	[28]
PVDF	Surface modified/hydrophilization using interfacial polymerization of nylon 6,6	193	[15]
PAN	Phase-inverted chitosan layer	203	[29]
PEI	Functionalized carbon nanotubes	310	[30]
PSf/PAN	–	340	[31]

Table 5
Co-current PRO and FO performance of FO membranes using real seawater as a feed solution

Mode	J_W (LMH)	Feed solution	Initial feed solution concentration	Time
Co-current FO	15.11	Seawater	2 M NaCl	3 h
Co-current PRO	49.44	Seawater	2 M NaCl	3 h

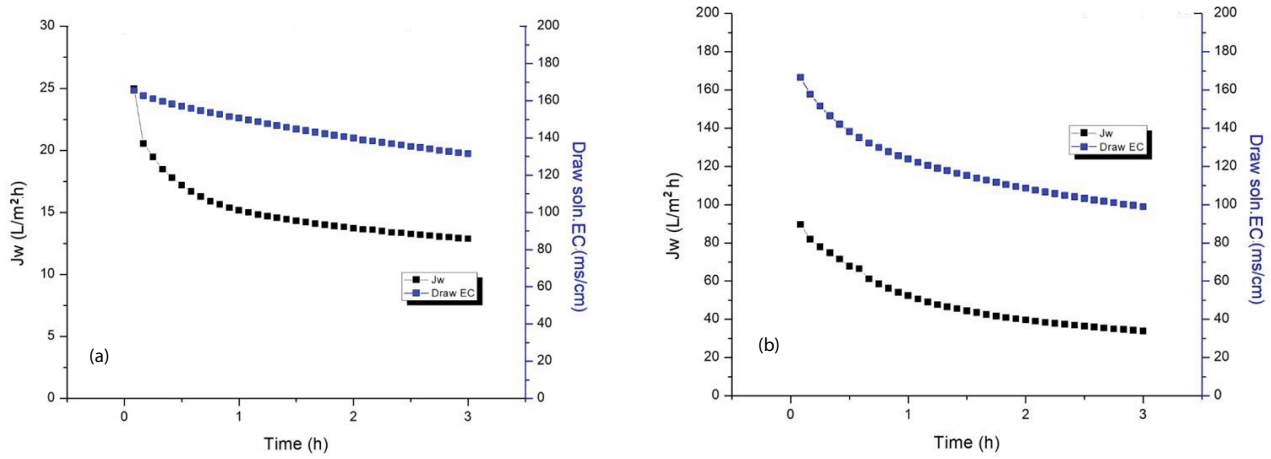

Fig. 5. Water flux of fabricated membranes at (a) co-current FO mode and (b) co-current PRO mode, using real seawater (15.77 ms/cm) and 2 M NaCl as a feed solution and draw the solution, respectively.

draw solution concentration refers essentially to the effect of water permeation from the feed side to the draw side and to a lesser extent for the reverse salt flux in the opposite direction.

Wang et al. [16] refer the water flux difference between PRO and FO modes to the decreased of effective driving force which could be resulted from severer dilutive ECP within the boundary layer at the membrane surface and/or ICP within the substrate layer due to the salt leakage from the draw solution to the feed. In this study, the water flux in the FO mode is high enough to exclude that the ICP has a crucial role in the effective driving force reduction. For this reason, the big difference in water flux between FO and PRO is most likely because of the dilutive ECP at the surface of the separation layer.

Looking at Table 6, the water flux ratio between PRO and FO (named water flux ratio$^{PRO/FO}$) decreased from 4.82 to 3.28 as the distilled water was replaced by seawater in the feed side. The reduction of the water flux ratio$^{PRO/FO}$ refers generally to concentration polarization, but the water flux ratio$^{PRO/FO}$ in the case of seawater still high enough. This again suggests that ICP has a limited effect on this membrane water flux as a result of its low substrate S-value.

In both studies [16] and [32], a more pronounced leveling of the water flux ratio$^{PRO/FO}$ occurred with the replacement of

Table 6
Comparison of FO membrane performance among this study membrane and other studies using deionized water and seawater (modified from [16])

Membranes	Water flux (PRO/FO) (LMH)	Water flux (PRO/FO ratio)	Reverse salt flux (PRO/FO) (gMH)	Draw solution	Feed solution	References
sPSf FO	313/65	4.81		1.0 M NaCl	Deionized water	This study
sPSf FO flat-sheet	49.44[b]/15.11[a]	3.3		2.0 M NaCl	–1.1 wt.% NaCl	This study
Polyethersulfone (PES)/sPSf FO flat-sheet	47.5/26.0	1.83	12.4/8.3	2.0 M NaCl	Deionized water	[16]
Polyethersulfone (PES)/sPSf FO flat-sheet	12.7/11.8	1.07	–	2.0 M NaCl	3.5 wt.% NaCl	[16]
PES-co-sPSf FO flat-sheet	15/13.5	1.11	–	2.0 M NaCl	3.5 wt.% NaCl	[14]
#C-FO hollow fiber	68.0/29.5	2.3	5.8/2.6	2.0 M NaCl	Deionized water	[32]
#C-FO hollow fiber	12.4/12.4	1	–	2.0 M NaCl	3.5 wt.% NaCl	[32]
Hydration Technology Innovations LLC flat sheet membrane	13.0 (FO)	–	–	2.0 M NaCl	Deionized water	[19]
Hydration Technology Innovations LLC flat sheet membrane	11.2 (PRO)	–	–	2.0 M NaCl	3.5 wt.% NaCl	[33]

[a]done at co-current FO; [b]done at counter-current PRO.

Table 7
Co-current PRO and FO performance of FO membranes using model seawater (NaCl) feed solution

Mode	J_W (LMH) over 3 h	Feed solution	Initial draw solution	Time
Co-current FO	7.97	15.77 ms/cm NaCl synthetic solution	2 M NaCl	3 h
Counter current FO	21.65	15.77 ms/cm NaCl synthetic solution	2 M NaCl	3 h
Co-current PRO	53.8	15.77 ms/cm NaCl synthetic solution	2 M NaCl	3 h
Counter current PRO	92.40	15.77 ms/cm NaCl synthetic solution	2 M NaCl	3 h

distilled water by seawater as it decreased from 1.83 to 1.07 and from 2.3 to 1.

3.3.2. Performance of FO membrane using synthetic solutions as feed water

Another sample was prepared from a new fabricated membrane to find the performance of the membrane using synthetic solutions. NaCl and $MgSO_4$ feed solutions with a salinity of 15.77 ms/cm prepared in the laboratory to simulate the salinity of the seawater sample taken from the Bosphorus bay, Istanbul. The same operating conditions that were used to characterize membrane desalination performance against real seawater were applied. To get an insight into the effect of flux hydrodynamics, in addition to FO/PRO co-current flow configuration, the membrane performance characterized also against FO/PRO counter current. The results in Table 7 and Table 8 showed an obvious upswing in water flux when FO/PRO counter-current mode applied to compare to FO/PRO co-current mode.

No major variations in membrane efficiency have been found between the various forms of synthetic solutions

Table 8
Co-current PRO and FO performance of FO membranes using model seawater ($MgSO_4$) feed solution

Mode	J_W (LMH) over 3 h	Feed solution	Initial draw solution	Time
Co-current FO	10.37	15.77 ms/cm $MgSO_4$ synthetic solution	2 M NaCl	3 h
Counter current FO	10.12	15.77 ms/cm $MgSO_4$ synthetic solution	2 M NaCl	3 h
Co-current PRO	45.64	15.77 ms/cm $MgSO_4$ synthetic solution	2 M NaCl	3 h
Counter current PRO	–	15.77 ms/cm $MgSO_4$ synthetic solution	2 M NaCl	3 h

(NaCl and $MgSO_4$) on the one side and the contrast between natural and synthetic solutions on the other. Han et al. [34] developed a TFC-FO membrane of sulfonated polyether ketone (SPEK) based substrate for desalination. The casted substrate comprising 50 wt.% SPEK. The membrane exhibited a water flux of 50 LMH against DIO and 22 LMH against the 3.5 wt.% NaCl synthetic solution, respectively, when using 2 M NaCl as the DS measured under the PRO mode. While, in our case, the membrane showed a water flux of 53.8 LMH against 15.77 ms/cm NaCl synthetic solution using 2 M NaCl as the DS measured under the PRO mode.

With this superior flux, especially in the counter current PRO mode (92.40 MLH), it is worthwhile stating that membrane not only has a great potential in seawater desalination but also it is promising for energy production via pressure-retarded osmosis technology.

4. Conclusion

The re-design and alteration of the support layer structure/material in the FO membranes, with a low *S*-value and high hydrophilicity, may play a crucial role in limiting the ICP effect. Furthermore, it can give more flexibility to manipulate the thickness of the skin separation layer to enhance the selectivity without highly compromise the flux.

In this study, the sPSf electro-spun nanofiber mat, with unique scaffold structure and hydrophilicity, is used for FO membrane substrate fabrication. The potential use of the fabricated membrane for the application of seawater desalination is investigated. The newly developed membrane showed a high desalination throughput and a small structural parameter value. The membranes with high *S*-value would show a more leveled variance of the water flux ratio$^{PRO/FO}$, which could be reached to the unity, as the feed solution changed from DIO to seawater. The results demonstrated that the membrane used in this study still has a significant flux ratio$^{PRO/FO}$ variance when applied for real seawater. In addition to the structural parameter, the water flux ratio$^{PRO/FO}$ variance between pure water flux and seawater flux could be considered another performance indicator of the FO membranes regarding the ICP effect.

The significant increase of the salinity in the feed side during the seawater experiment suggests that solution concentration, in general, could be a potential application of the membrane developed by this work.

Acknowledgment

The authors are grateful to TUBITAK (The Scientific and Technological Research Council of Turkey) for their financial support under the grant (Project No: 113Y356).

Symbols

A	—	Water permeability, m s^{-1} atm^{-1}
B	—	Solute permeability, m s^{-1}
J_W	—	Water flux, LMH
J_S	—	Reverse salt flux, gMH
S	—	Membrane structure parameter, m
J_W/J_S	—	Reverse flux selectivity

Subscripts

FO	—	Forward osmosis mode
PRO	—	Pressure retard mode
FS	—	Feed solution
DS	—	Draw solution
ICP	—	Internal concentration polarization
ECP	—	External concentration polarization
CFV	—	Cross flow velocity
SR	—	Salt rejection
TFC	—	Thin-film composite
RO	—	Reverse osmosis
sPSf	—	Sulfonated polysulfone
PAN	—	Polyacrylonitrile
PVDF	—	Polyvinylidene fluoride
PEI	—	Polyethylenimine
DIO	—	Deionized water
LMH	—	Liter per square meter hour
gMH	—	Gram per square meter hour

References

[1] M.A. Shannon, P.W. Bohn, M. Elimelech, J.G. Georgiadis, B.J. Mariñas, A.M. Mayes, Science and technology for water purification in the coming decades, Nature, 452 (2008) 301–310.
[2] J.E. Cadotte, Chapter 12 – Evolution of Composite Reverse Osmosis Membranes, D.R. Lloyd, Ed., Materials Science of Synthetic Membranes, Washington DC, ACS, 1985, pp. 273–294.
[3] M.F. Jimenez-Solomon, P. Gorgojo, M. Munoz-Ibanez, A.G. Livingston, Beneath the surface: influence of supports on thin film composite membranes by interfacial polymerization for organic solvent nanofiltration, J. Membr. Sci., 448 (2013) 102–113.
[4] S.S. Shenvi, A.M. Isloor, A.F. Ismail, A review on RO membrane technology: developments and challenges, Desalination, 368 (2015) 10–26.
[5] I.L. Alsvik, M.B. Hägg, Preparation of thin film composite membranes with polyamide film on hydrophilic supports, J. Membr. Sci., 428 (2013) 225–231.
[6] T.T. Ni, Q.C. Ge, Highly hydrophilic thin-film composition forward osmosis (FO) membranes functionalized with aniline sulfonate/bisulfonate for desalination, J. Membr. Sci., 564 (2018) 732–741.
[7] C. Ding, X. Zhang, L. Shen, J. Huang, A. Lu, F.R. Zhong, Y. Wang, Application of polysaccharide derivatives as novel draw solutes in forward osmosis for desalination and protein concentration, Chem. Eng. Res. Des., 146 (2019) 211–220.
[8] S.M. Iskander, J.T. Novak, Z. He, Enhancing forward osmosis water recovery from landfill leachate by desalinating brine and recovering ammonia in a microbial desalination cell, Bioresour. Technol., 255 (2018) 76–82.
[9] Z.L. Cheng, X. Li, T.-S. Chung, The forward osmosis-pressure retarded osmosis (FO-PRO) hybrid system: a new process to mitigate membrane fouling for sustainable osmotic power generation, J. Membr. Sci., 559 (2018) 63–74.
[10] T.-S. Chung, L. Luo, C.F. Wan, Y. Cui, G. Amy, What is next for forward osmosis (FO) and pressure retarded osmosis (PRO), Sep. Purif. Technol., 156 (2015) 856–860.
[11] ForwardOsmosisTech, Guide to Forward Osmosis Membranes, Retrieved September 10, 2019. Available at: http://www.forwardosmosistech.com/forward-osmosis-membranes/
[12] M.Y. Park, J.J. Lee, S. Lee, J.H. Kim, Determination of a constant membrane structure parameter in forward osmosis processes, J. Membr. Sci., 375 (2011) 241–248.
[13] J.R. McCutcheon, M. Elimelech, Influence of membrane support layer hydrophobicity on water flux in osmotically driven membrane processes, J. Membr. Sci., 318 (2008) 458–466.
[14] N. Widjojoa, T.-S. Chunga, M. Weber, C. Maletzko, V. Warzelhan, A sulfonated polyphenylenesulfone (sPPSU) as the

supporting substrate in thin film composite (TFC) membranes with enhanced performance for forward osmosis (FO), Chem. Eng., 220 (2013) 15–23.
[15] L.W. Huang, J.T. Arena, J.R. McCutcheon, Surface modified PVDF nanofiber supported thin film composite membranes for forward osmosis, J. Membr. Sci., 499 (2016) 352–360.
[16] K.Y. Wang, T.-S. Chung, G. Amy, Developing thin-film-composite forward osmosis membranes on the PES/sPSf substrate through interfacial polymerization, AlChE J., 58 (2012) 770–781.
[17] J.R. McCutcheon, M. Elimelech, Influence of concentrative and dilutive internal concentration polarization on flux behavior in forward osmosis, J. Membr. Sci., 284 (2006) 237–247.
[18] C. Klaysom, T.Y. Cath, T. Depuydt, I.F.J. Vankelecom, Forward and pressure retarded osmosis: potential solutions for global challenges in energy and water supply, Chem. Soc. Rev., 42(16) (2013) 6959–89.
[19] W.A. Phillip, J.S. Yong, M. Elimelech, Reverse draw solute permeation in forward osmosis: modeling and experiments, Environ. Sci. Technol., 44 (2010) 5170–5176.
[20] R.M. El Khaldi, M.E. Pasaoglu, S. Guclu, Y.Z. Menceloglu, R. Ozdogan, M. Celebi, M.A. Kaya, I. Koyuncu, Fabrication of high-performance nanofiber-based FO membrane, Desal. Water Treat., 147 (2019) 56–72.
[21] J.S. Yong, W.A. Phillip, M. Elimelech, Coupled reverse draw solute permeation and water flux in forward osmosis with neutral draw solutes, J. Membr. Sci., 392–393 (2012) 9–17.
[22] J.T. Arena, S.S. Manickam, K.K. Reimund, P. Brodskiy, J.R. McCutcheon, Characterization and performance relationships for a commercial thin film composite membrane in forward osmosis desalination and pressure retarded osmosis, Ind. Eng. Chem., 54 (2015) 11393–11403.
[23] ForwardOsmosisTech, *S*-value Calculator for Forward Osmosis Membranes, Retrieved September 10, 2019. Available at: https://www.forwardosmosistech.com/s-value-calculator-for-forward-osmosis-membranes/
[24] N.-N. Bui, J.R. McCutcheon, Nanoparticle-embedded nanofibers in highly permselective thin-film nanocomposite membranes for forward osmosis, J. Membr. Sci., 518 (2016) 338–346.
[25] L. Shen, X. Zhang, L. Tian, Z. Li, C. Ding, M. Yi, C. Han, X. Yu, Y. Wang, Constructing substrate of low structural parameter by salt induction for high-performance TFC-FO membranes, J. Membr. Sci., 600 (2020) 117866.
[26] M.J. Park, R.R. Gonzales, A. Abdel-Wahab, S. Phuntsho, H.K. Shon, Hydrophilic polyvinyl alcohol coating on hydrophobic electrospun nanofiber membrane for high performance thin film composite forward osmosis membrane, Desalination, 426 (2018) 50–59.
[27] S.-F. Pan, Y.C. Dong, Y.-M. Zheng, L.-B. Zhong, Z.-H. Yuan, Self-sustained hydrophilic nanofiber thin film composite forward osmosis membranes: preparation, characterization and application for simulated antibiotic wastewater treatment, J. Membr. Sci., 523 (2017) 205–215.
[28] A.A. Shah, Y.H. Cho, S.-E. Nam, A. Park, Y.-I. Park, H. Park, High performance thin-film nanocomposite forward osmosis membrane based on PVDF/bentonite nanofiber support, J. Ind. Eng. Chem., 86 (2020) 90–99.
[29] J. Shi, H. Kang, N. Li, K.Y. Teng, W.Y. Sun, Z.W. Xu, X.M. Qian, Q. Liu, Chitosan sub-layer binding and bridging for nanofiber-based composite forward osmosis membrane, Appl. Surf. Sci., 478 (2019) 38–48.
[30] M. Tian, Y.-N. Wang, R. Wang, Synthesis and characterization of novel high-performance thin film nanocomposite (TFN) FO membranes with nanofibrous substrate reinforced by functionalized carbon nanotubes, Desalination, 370 (2015) 79–86.
[31] S. Shokrollahzadeh, S. Tajik, Fabrication of thin film composite forward osmosis membrane using electrospun polysulfone/polyacrylonitrile blend nanofibers as porous substrate, Desalination, 425 (2018) 68–76.
[32] S.R. Chou, L. Shi, R. Wang, C.Y. Tang, C.Q. Qiu, A.G. Fane, Characteristics and potential applications of a novel forward osmosis hollow fiber membrane, Desalination, 261 (2010) 365–372.
[33] J.R. McCutcheon, R.L. McGinnis, M. Elimelech, Desalination by ammonia–carbon dioxide forward osmosis: influence of draw and feed solution concentrations on process performance, J. Membr. Sci., 278 (2006) 114–123.
[34] G. Han, T.-S. Chung, M. Toriida, S. Tamai, Thin-film composite forward osmosis membranes with novel hydrophilic supports for desalination, J. Membr. Sci., 423–424 (2012) 543–555.